Unipolar resistive switching effect in $YMn_{1-\delta}O_3$ thin films

Z. B. Yan, S. Z. Li, K. F. Wang, and J.-M. Liu[a)]
Nanjing National Laboratory of Microstructures, Nanjing University, Nanjing 210093, People's Republic of China and International Center for Materials Physics, Chinese Academy of Sciences, Shenyang 110016, People's Republic of China

(Received 19 October 2009; accepted 9 December 2009; published online 5 January 2010)

Steady unipolar resistive switching of $Pt/YMn_{1-\delta}O_3/Pt$ MIM structure is investigated. High resistance ratio ($>10^4$) of high resistance state (HRS) over low resistance state (LRS) and long retention ($>10^5$ s) are achieved. It is suggested that the Joule heating and Poole–Frenkel effect dominate respectively the conduction of the LRS and HRS in high electric field region. The resistive switching is explained by the rupture and formation of conductive filaments in association with the local Joule-heat-induced redox inside $YMn_{1-\delta}O_3$. © *2010 American Institute of Physics*. [doi:10.1063/1.3280380]

Recently, reversible resistive switching (RS) in transition-metal oxides has attracted a great deal of interests for its potential applications in nonvolatile resistance random access memory devices.[1–8] The resistance of these materials can be switched between a high resistance state (HRS) and a low resistance state (LRS) by electric field with either opposite polarity (bipolar) or different magnitude (unipolar).[1,2] The unipolar RS, which has been intensively studied due to some advantages in device performance, can be well understood by a model based on the formation/rupture of conductive filaments in insulating matrix.[1–8] For some metal-insulator-metal (MIM) structures, the conductive filaments may be composed of the electrode metals transported into the insulator, while for others the decomposed insulator materials such as conductive sub-oxides play as the filaments.[7–9] Hence, exploring the unipolar RS mechanisms for various oxides materials is important to seek the good performance for future applications.

The priority and advantage of ferroelectric (FE) materials as bipolar RS media were addressed,[10] while few investigation on unipolar RS of ferroelectrics has been reported. $YMnO_3$ is a FE material with a hexagonal structure at room temperature and also with multiferroicity.[11] Since the charge vacancies at Mn-site may contribute substantially to the leakage current, such structural defects[12] or inhomogeneous chemical states[5] induced by the vacancies may also allow space for the unipolar RS effect. Here we study the unipolar RS effect of Mn-deficient $YMnO_3$ ($YMn_{1-\delta}O_3$) and discuss the conduction behaviors at the LRS and HRS. The reliable and stable unipolar RS characteristics of the $Pt/YMn_{1-\delta}O_3/Pt$ MIM structure will be demonstrated.

The $YMn_{1-\delta}O_3$ thin films were deposited on (111) $Pt/TiO_2/SiO_2/Si$ substrates by pulsed laser deposition using a KrF excimer laser with wavelength of 248 nm. The laser energy density, laser repetition rate, oxygen ambient pressure, and growth temperature are 3 J/cm^2, 3 Hz, 18 Pa, and 800 °C, respectively. The as-grown samples were then *in situ* annealed at the same temperature under an oxygen atmosphere of 100 Pa. X-ray diffraction (XRD) indicates that the films were polycrystalline, as shown in Fig. 1(a). Scanning electron microscopy (SEM) and x-ray photoelectron spectroscopy (XPS) were used to probe the thickness and chemical bonding states of $YMn_{1-\delta}O_3$ films, respectively. The $YMn_{1-\delta}O_3$ thin films of 150 and 300 nm in thickness were prepared for various purposes.

The Pt top electrodes with 100 and 200 μm in diameter were deposited by rf magnetron sputtering with a shadow mask. The resistive memory unit with the films of 300 nm and 150 nm in thickness are labeled as unit-A and unit-B, respectively. All the current-voltage (*I-V*) characteristics were measured by the two-probe method using a Keithley 236 source meter, in which the pulsed voltage sweeps were applied with a pulse width of 10 ms and a pulse separation of 10 ms.

The fresh memory units are always at HRS with a resistance of ~10 MΩ. To obtain the reversible RS behavior, a "forming" process is needed. Figure 1(b) shows the measured *I-V* curves for unit-A. Starting from HRS, a positive voltage sweep ($0 \rightarrow 20$ V) with a current compliance of 20 mA triggers the conduction abruptly at the forming voltage or the set voltage (V_{set}), and the unit switches from HRS to LRS (denoted as forming or SET processes, separately). Afterwards, another voltage sweep ($0 \rightarrow 2$ V) causes the abrupt decrease of current at the reset voltage (V_{reset}) and the unit switches back to HRS (denoted as RESET process). For negative voltage sweeps ($0 \rightarrow -20$ V) and ($0 \rightarrow -2$ V) in sequence, the similar SET and RESET processes are observed. The polarity independence of the SET and RESET transi-

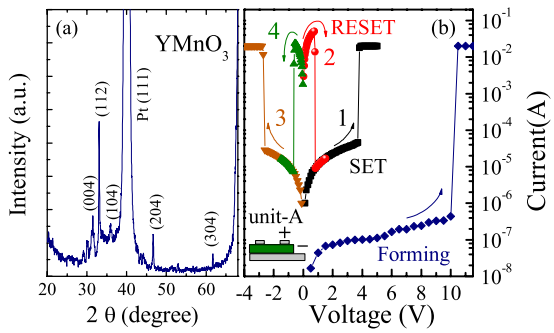

FIG. 1. (Color online) (a) XRD spectrum of the $YMn_{1-\delta}O_3$ film. (b) Current-voltage (*I-V*) data of unit-A. Inset: the configuration of unit-A, 300 nm $YMn_{1-\delta}O_3$ film.

a)Electronic mail: liujm@nju.edu.cn.

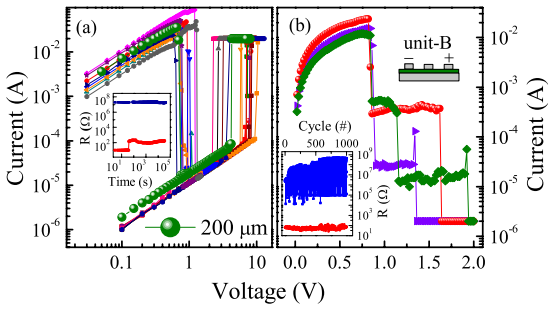

FIG. 2. (Color online) (a) *I-V* curve in switching of ten cycles. Inset: the retentions of both LRS and HRS, readout at 0.1 V. The olive circle dots are measured with top electrode of 200 μm in diameter, while others with top electrode of 100 μm in diameter. (b) *I-V* data of unit-B (150 nm $YMn_{1-\delta}O_3$ film). Inset: Endurances of unit-B, readout at 0.1 V.

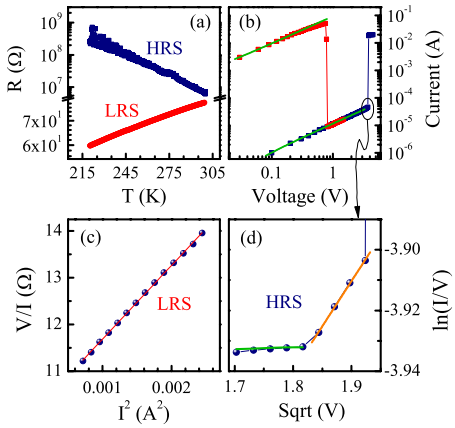

FIG. 3. (Color online) (a) *R-T* dependence of both HRS and LRS. (b) The log *I*-log *V* plot of unit-A, with the green lines fitted by the ohmic law. (c) Measured V/I as a function of I^2 at the LRS in high field region (0.3 $\rightarrow$0.75 V). (d) $\ln(I/V)$ as a function of $V^{1/2}$ at the HRS in high field region (2.9$\rightarrow$3.8 V).

tions and nearly symmetric *I-V* characteristics indicate the unipolar RS characteristics.

To proceed, the *I-V* characteristics with ten consecutive cycles are shown in Fig. 2(a). The SET and RESET transitions typically occur at $V_{set}\sim 2.2-10$ V and $V_{reset}\sim 0.6-1.3$ V, respectively. The retentions of HRS and LRS over $\sim 10^5$ s are maintained and the resistance ratio, R_{HRS}/R_{LRS}, readout at 0.1 V, is $\sim 10^5$, as shown in the inset of Fig. 2(a). These properties demonstrate that $YMn_{1-\delta}O_3$ is a promising candidate for resistive memory applications.

In order to understand the switching mechanisms, we perform the RS cycle on a larger top electrode (200 μm in diameter). It is seen from Fig. 2(a) that $V_{set}\sim 4.2$ V and $V_{reset}\sim 0.7$ V, still in the range of 2.2–10 V and 0.6–1.3 V, respectively. That is to say that both V_{set} and V_{reset} do not significantly depend on the size of top electrode, suggesting the presence of local conducting filaments for the present unipolar RS.[2,4,7]

To further check the formation and rupture of local conductive filaments as the dominant mechanism of the RS sequence, the *I-V* characteristics of the two capacitors in series are measured. We measure unit-B with top electrode of 100 μm in diameter, as shown in the inset of Fig. 2(b). Note that the thickness of $YMn_{1-\delta}O_3$ film in unit-B is a half of that in unit-A ($\sim$300 nm). Unit-B can be regarded as modified unit-A by inserting a Pt layer into the middle of the 300 nm thick $YMn_{1-\delta}O_3$ film, i.e., unit-B is comprised of two Pt/$YMn_{1-\delta}O_3$ (150 nm)/Pt capacitors in series. This insertion into a network of conductive filaments sandwiched between two terminal electrodes enhances the connectivity. The possibility to find multiple conductive filaments between the two top electrodes in unit-B is higher than that in unit-A. Given the presence of these filaments, the current mainly concentrates on those filaments of the lowest resistance during the voltage sweeping from 0$\rightarrow$2 V. As a result, remarkable local Joule heating may lead to the local redox and the rupture of these filaments at V_{reset}, and the current is redistributed onto those filaments of the second lowest resistance. Subsequently, the rupture of these filaments may take place at a higher voltage.

Given this mechanism in operation, multistep RS sequence should be observed during the RESET in unit-B, as evidenced in Fig. 2(b), noting that the measurement was performed with the same voltage sweep on unit-A (0$\rightarrow$2 V for RESET, and 0$\rightarrow$20 V with a compliance current of 20 mA for SET). In addition, the LRS/HRS endurance over 10^3 cycles and the HRS fluctuations over three orders of magnitude in unit-B, given the readout at 0.1 V, are also illustrated in the inset of Fig. 2(b). We observe that for unit-B, the endurance is much better and the HRS fluctuations are much larger than those for unit-A (not shown here). Therefore, by associating the behavior of the two-state switches in unit-A with that of the multiple-state switches in unit-B, the filamentary model can be a good approach to the reversal RS effect in the Pt/$YMn_{1-\delta}O_3$/Pt device.

We also carried out additional three-terminal experiments to identify the sites the RS occurs. The experimental steps are as follows: (1) switch to the HRS after the "forming" process, with one top electrode (TE-I) as anode and another top electrode (TE-II) as cathode, indicating that the filament between the two top electrodes is ruptured; (2) read the resistive states R_1 and R_2 with small voltage respectively between the TE-I and bottom electrode and between the TE-II and bottom electrode. Our data (not shown here) indicate that sometimes R_1 is in the HRS while R_2 is in the LRS, and sometimes on the contrary. That is to say, the filament rupture in the anode side or in the cathode side should not be a major sequence. In other words, the unipolar RS in Pt/$YMn_{1-\delta}O_3$/Pt memory unit should not occur near the anode or cathode but inside the $YMn_{1-\delta}O_3$ film.

For checking the performance and understanding the mechanism of the RS effect, several aspects of the related physics can be addressed. First, the temperature (T) dependence of the HRS and LRS is measured at a rate of 2 K/min and the results are shown in Fig. 3(a). For the LRS, resistance $R(T)$ decreases with decreasing T, indicating the metallic state, while the HRS is an insulating/semiconducting state from the $R(T)$ character.

Second, one can investigate the conduction modes for the LRS and HRS from the *I-V* characteristics,[4,7,13] and the results for unit-A are presented in Fig. 3(b). In the low voltage region, the *I-V* characteristics for both HRS and LRS exhibit the Ohmic behavior, indicating the dominant Ohmic conduction. In the high voltage region (0.3$\rightarrow$0.75 V), the *I-V* data for the LRS deviate from the Ohmic behavior. Since the LRS is metallic, resistance $R(T)$ can be expressed as: $R(T)=R_0[1+\beta(T-T_0)]$, where β is the temperature coefficient, T_0 is a reference temperature, and R_0 is the resistance

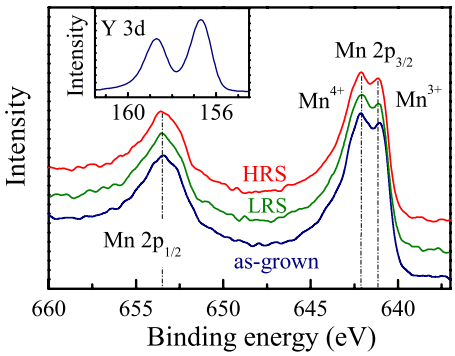

FIG. 4. (Color online) XPS spectrums of Mn $2p$ when the $YMn_{1-\delta}O_3$ film is as-grown, at LRS, and at HRS respectively. Inset: XPS spectra of Y $3d$.

at T_0. The current flowing through the filaments generates the Joule heating with the power $I^2R(T)$, raising T in the local region accordingly. As an approximation, one has $R \propto T$ and $T \propto I^2$ lead to $V/I \propto I^2$.[14,15] This dependence receives confirmation from experiment, as shown in Fig. 3(c), clearly indicating that the Joule heating effect dominates the electrical prosperity of LRS in the high voltage region.

As for the HRS, the linear dependence of $\ln(I/V)$ on $V^{1/2}$ in Fig. 3(d) clearly shows two types of transport modes. At $V < 3.2$ V, the low field region, the independence of $\ln(I/V)$ on $V^{1/2}$ indicates the ohmic behavior. For the high field region ($3.2 \rightarrow 3.8$ V), the linear dependence suggests that the conduction mechanism is the Poole–Frenkel emission,[4,7,8,13] a bulk effect, which comes from a lowering of the coulomb potential barrier of a trap site due to electric field,[13] indicating that the conduction of the HRS in the high field region is governed by electron hopping between the trap states probably existing on grain boundaries or structural defects induced by Mn vacancies.[7]

To detect the film composition and detect the valance variation after the RS occurs, the XPS data of the as-grown YMO films and the data in the regions with the HRS or LRS were measured, as shown in Fig. 4. For the XPS measurement on the regions with the HRS or LRS, the HRS or LRS was obtained in prior to the XPS probing, by a voltage-sweep with a Pt probe as an anode directly touching onto the top surface of $YMn_{1-\delta}O_3$ film. There are two peaks in the core level spectra of Mn $2p_{3/2}$ for all cases. One is at ~642.1 eV assigned to Mn^{4+}, and the other is at ~641.2 eV owing to Mn^{3+}.[16] The similar spectra of Mn $2p_{3/2}$ for all cases indicate no detectable variation of Mn valance at the film surface after the RS event, consistent with the above conclusion that the RS does not occur near the anode. It should be noted that the XPS probed atomic ratio of Mn/Y, is ~0.9 for all samples, smaller than the stoichiometric value. This indicates the deficiency of Mn in the films with respect to Y and the film is $YMn_{1-\delta}O_3$.

Finally, we discuss the possible origin of unipolar RS in $YMn_{1-\delta}O_3$ film. Under a high electric field, the soft breakdown leads to the formation of conductive filaments probably on the structural defects induced by Mn vacancies.[2,5] On the other hand, the remarkable local Joule heating in the less conductive region of the conductive filaments will lead to the local redox, causing to the rupture of filament. According to the coexistence conditions estimated from thermodynamic data,[17] Mn^{4+} in the manganites may possibly reduce to Mn^{3+} above 800 K. Given that the existence of Mn vacancies and the spatially inhomogeneity of the chemical states inside the $YMn_{1-\delta}O_3$ films may allow a much lower T for the local redox in the nanoscale region, the Joule-heat-induced reduction of Mn^{4+} back to Mn^{3+} in the less conductive region is possible. This process seems to be one of the reasons for the metal-to-insulator transitions, featured with the rupture of the filament. Nevertheless, these arguments need more delicate experiments on the microstructures and transport in microscopic level, which are technically challenging.

In summary, we have reported the unipolar RS behavior of $Pt/YMn_{1-\delta}O_3/Pt$ MIM structure at room temperature. The reversible RS with high resistance ratio and long retention has been demonstrated. In high electric field region, the Joule heating effect and the Poole–Frenkel emission dominate the conduction of the LRS and HRS, respectively. This interesting RS behavior can be explained by generation and rupture of conductive filaments. The RS occurs not at the electrode interface but at the regions where the conduction is weak and the redox may take place due to the remarkable local Joule heating. This work implies that $YMn_{1-\delta}O_3$ can be a promising candidate as memristor.

This work was supported by the Natural Science Foundation of China (Grant Nos. 50832002 and 10874075), the National Key Projects for Basic Researches of China (Grant Nos. 2006CB921802 and 2009CB623303), and the Research Project of Jiangsu Province, China (Grant No. BK2008024).

[1] R. Waser, R. Dittmann, G. Staikov, and K. Szot, Adv. Mater. **21**, 2632 (2009).
[2] A. Sawa, Mater. Today **11**, 28 (2008).
[3] W. Y. Chang, J. H. Liao, Y. S. Lo, and T. B. Wu, Appl. Phys. Lett. **94**, 172107 (2009).
[4] W. Y. Chang, Y. C. Lai, T. B. Wu, S. F. Wang, F. Chen, and M. J. Tsai, Appl. Phys. Lett. **92**, 022110 (2008).
[5] R. Yasuhara, K. Fujiwara, K. Horiba, H. Kumigashira, M. Kotsugi, M. Oshima, and H. Takagi, Appl. Phys. Lett. **95**, 012110 (2009).
[6] Z. B. Yan, K. F. Wang, S. Z. Li, S. J. Luo, and J.-M. Liu, Appl. Phys. Lett. **95**, 143502 (2009); Z. B. Yan, S. Dong, K. F. Wang, C. L. Lu, F. Gao, and J.-M. Liu, J. Appl. Phys. **104**, 013916 (2008).
[7] K. Nagashima, T. Yanagida, K. Oka, and T. Kawai, Appl. Phys. Lett. **94**, 242902 (2009).
[8] J. W. Seo, J. W. Park, K. S. Lim, J. H. Yang, and S. J. Kang, Appl. Phys. Lett. **93**, 223505 (2008).
[9] M. Kawai, S. Inoue, M. Mizumaki, N. Kawamura, and Y. Shimakawa, and Y. Shimakawa1, Appl. Phys. Lett. **94**, 082102 (2009).
[10] V. Garcia, S. Fusil, K. Bouzehouane, S. Enouz-Vedrenne, N. D. Mathur, A. Barthélémy, and M. Bibes, Nature (London) **460**, 81 (2009); J. Rodríguez Contreras, H. Kohlstedt, U. Poppe, R. Waser, C. Buchal, and N. A. Pertsev, Appl. Phys. Lett. **83**, 4595 (2003).
[11] K. F. Wang, J.-M. Liu, and Z. F. Ren, Adv. Phys. **58**, 321 (2009).
[12] C. Park, S. H. Jeon, S. C. Chae, S. Han, B. H. Park, S. Seo, and D.-W. Kim, Appl. Phys. Lett. **93**, 042102 (2008).
[13] J. S. Choi, J.-S. Kim, I. R. Hwang, S. H. Hong, S. H. Jeon, S.-O. Kang, B. H. Park, D. C. Kim, M. J. Lee, and S. Seo, Appl. Phys. Lett. **95**, 022109 (2009).
[14] S. B. Lee, S. C. Chae, S. H. Chang, and T. W. Noh, Appl. Phys. Lett. **94**, 173504 (2009).
[15] S. H. Chang, J. s. Lee, S. C. Chae, S. B. Lee, C. Liu, B. Kahng, D. W. Kim, and T. W. Noh, Phys. Rev. Lett. **102**, 026801 (2009).
[16] H. W. Nesbitt and D. Banerjee, Am. Mineral. **83**, 305 (1998).
[17] I. Barin, *Thermochemical Data of Pure Substances*, 3rd ed. (VCH, Weinheim, 1995).